Design of an Edge Filter Based on a Phase-Only Modulated Long-Period Fiber Grating

Hua Zhao
Chengliang Zhu
Hongpu Li, *Member, IEEE*
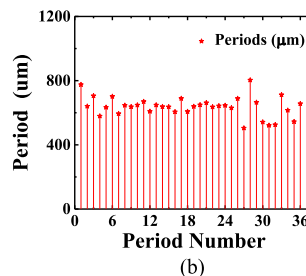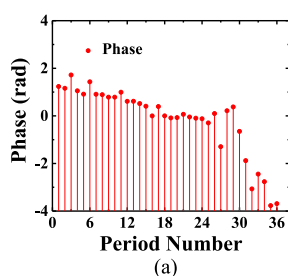
♦IEEE

Design of an Edge Filter Based on a Phase-Only Modulated Long-Period Fiber Grating

Hua Zhao [1], **Chengliang Zhu,** [2] **and Hongpu Li** [2], ***Member, IEEE***

[1]Key Laboratory of Optoelectronic Technology of Jiangsu Province, School of Physical Science and Technology, Nanjing Normal University, Nanjing 210023, China
[2]Faculty of Engineering, Shizuoka University, Hamamatsu 432-8561, Japan

Abstract: An efficient edge filter with an ultrabroad dynamic range is first proposed and numerically demonstrated, which is achieved by using a phase-only modulated long-period fiber grating (LPG). As a typical design example, an edge filter with a linear dynamic range of ∼50 nm in wavelength and ∼85% in transmission loss has been successfully obtained, which are the best results reported to date among those of the fiber grating based edge filters. Fabrication tolerance analyses for the designed filter have also been performed. The simulation results show that the designed filter can be practically fabricated according to the position accuracy ($\pm$1.5 μm) of the current LPG's fabrication platform.

Index Terms: Edge filter, long-period fiber grating (LPG), phase-only modulation, genetic algorithm (GA).

1. Introduction

In past few decades, fiber grating-based sensors have been comprehensively studied and have been found wide applications in the fields of civil engineering, industry, biomedicine, chemistry, etc. [1]–[9]. To date, two common interrogation methods, i.e., the wavelength- and the power/intensity-interrogation approaches have mainly been utilized. For the first one, in order to precisely measure a wavelength shift, either an optical spectrum analyzer (OSA) with a high wavelength resolution or an extremely narrow line width tunable laser with both a wide tuning region and a high wavelength-scanning speed are desired. However, all of the devices mentioned above are extremely expensive, bulky, and thus not available for the practical applications. For the later one, an additional edge filter is generally desired, which can linearly convert the wavelength shift into a change in the optical power. Thus, only an optical power meter is needed for the edge filter-based interrogation method, which can provide more rapid, more compact, and more cost-effective system than the former one. However, an additional broad-band edge filter is essential and this kind of devices are extremely difficult to realize in optics. Until now, much effort trying to realize the optical edge filter have been made. In [10], Wei *et al.* have demonstrated a multimode fiber (MMF)-based edge filter and employed it to a fiber Bragg grating (FBG)-based temperature sensor. However, envelop of

the resulted spectrum is a sinusoidal one and moreover the dynamic ranges are limited to small quantities with just 2 nm in wavelength and 25% in transmission loss, respectively. Whereas in [11]–[13], edge filters had also been demonstrated by using either an erbium-doped fiber (EDF), or a long-period fiber grating (LPG), or a 1550/1570 WDM coupler. However, some additional components, such as the optical isolators/circulators, and couplers etc. are essential. To decrease the complexity of the power-interrogation system, an LPG-based edge filter had been proposed by Rao *et al.* [14], but the available linear-region obtained was just about 10 nm which is much less than the bandwidth (more than 30 nm) of the LPG itself. Dangui *et al.* had also proposed and demonstrated an ultra-broad band-rejection filter with a bandwidth (at 10 dB) larger than 360 nm, which is realized based on the utilization of a higher cladding mode-coupling in a LPG [15]. However, their research target was the ultra-broad band rather than the edge filter. Characteristics of the edge filter such as the dynamics ranges and the spectral linearity have not been considered. Later after the above, we have proposed and demonstrated a new kind of edge filter, which was realized based on a linearly chirped FBG [16]. Most recently, we have proposed and demonstrated a new power-interrogation method for simultaneous measurements of the temperature and torsion, which is based on the utilization of two cascaded helical-type LPGs [17]. However, the dynamic power range obtained was less than 6 dB (corresponding to a transmission-loss range of about 75%). Meanwhile the dynamic wavelength range obtained was less than 10 nm, which is still not large enough for some practical applications [11]–[14], [16], [17], especially for the case where the temperature change is larger than 250 °C and thus the real wavelength-shift happened in a LPG-based sensor may surpass this dynamic range. Therefore, to further develop an efficient edge filter with wide dynamic ranges is highly demanded even to date.

On the other hand, in the past few decades, much research attention has also been paid to the design of an optical edge filter. Bandyopadhyay *et al.* have proposed a method to design an edge filter [18], which is based on the utilization of an apodized linearly-chirped FBG. However, the dynamic range obtained are limited to 10 nm and 60% in wavelength and transmission loss, respectively. In [19] and [20], the authors have designed FBG-based triangular filters by using the genetic algorithm (GA) and the covariance-matrix adapted evolution algorithm, respectively, but dynamic range of the designed filters is just about 0.1 nm in wavelength. By employing the discrete layer peeling method, we had proposed a multichannel triangular filter for wavelength multiplexing interrogation [21]. However, due to the inherent narrow-bandwidth property of the FBG-based components, it is extremely difficult to obtain an edge filter that has wide dynamic ranges in both the wavelength and transmission loss, especially for the one with a wavelength range over 10 nm.

In this study, based on phase-only modulated LPG, an efficient and ultra-broad edge filter is firstly proposed and theoretically demonstrated. As a typical example, an edge filter that has linear dynamic ranges of ∼50 nm and ∼85% in wavelength and transmission loss, respectively, has been obtained. The designed results are the best ones reported to date among those fiber grating-based edge filters. Fabrication tolerances for the designed filter have also been analyzed.

2. Design Method for the Phase-Only Modulated LPG

2.1 Theory for Modeling a Conventional LPG

For a conventional LPG, its index change can be expressed as

$$\triangle n_s(z) = \triangle n_0 \left\{ 1 + m \cos \left(\frac{2\pi}{\Lambda_0} z + \varphi(z) \right) \right\}, \tag{1}$$

where z is the position along the grating. $\triangle n_0$, Λ_0, m, and $\varphi(z)$ are the maximum index-modulation, the central grating period, fringe visibility of the index change, and local phase of the grating, respectively. When all parameters of the LPG are known, its spectrum can be calculated by using the transfer matrix method (TMM) [22]. According to the TMM, the whole length of LPG is divided into many small sections with length $\triangle z$, and in each section, period of the grating and coupling coefficient κ are assumed to be constants. Hereafter, we define $R_j(\delta)$ and $S_j(\delta)$ as amplitudes of the

core and the cladding mode at end of the section j, then the transfer matrix F_j for the jth section can be defined by:

$$\begin{bmatrix} R_j(\delta) \\ S_j(\delta) \end{bmatrix} = F_j \begin{bmatrix} R_{j-1}(\delta) \\ S_{j-1}(\delta) \end{bmatrix}, \tag{2}$$

where

$$F_j = \begin{bmatrix} A_j & B_j \\ B_j & A_j^* \end{bmatrix}, A_j = cos(\gamma_j \Delta z) + i\delta sin(\gamma_j \Delta z)/\gamma_j$$

$$B_j = i\kappa_j sin(\gamma_j \Delta z)/\gamma_j,$$

and A_j^* represents the conjugate of A_j, $\gamma_j = \sqrt{\kappa_j^2 + \delta^2}$, and κ_j is the complex coupling-coefficient between the two coupled-modes in the jth section, which determines the local amplitude as well as the local phase of the grating. The detuning parameter δ is defined by:

$$\delta = (1/2)(\beta_{co} - \beta_{cl}^v) - \pi/\Lambda_0, \tag{3}$$

where β_{co}, β_{cl}^v are the propagation constants of the core mode and the vth cladding mode. The output fields then can be expressed by:

$$\begin{bmatrix} R_M(\delta) \\ S_M(\delta) \end{bmatrix} = F_M F_{M-1}...F_1 \begin{bmatrix} R_0(\delta) \\ S_0(\delta) \end{bmatrix}, \tag{4}$$

where the initial conditions of $R_0(\delta) = 1$ and $S_0(\delta) = 0$ are generally assumed and

$$F(\delta) = F_M F_{M-1}...F_1 = \begin{bmatrix} t(\delta) & c(\delta) \\ c(\delta) & t(\delta)^* \end{bmatrix}, \tag{5}$$

where $t(\delta)$ and $c(\delta)$ represent the transmission coefficients for core and cladding mode, respectively, which are also called the bar- and cross-transmission coefficients.

2.2 Phase-Only Modulated LPG

For a given target, the cross-transmission spectrum of $c(\delta)$, one can synthesize the coupling co-efficient $\kappa(z)$ of a LPG by directly using the discrete inverse-scattering algorithms [23]. However, for most of the synthesized gratings [23], [24], there exist either steep jumps or high-frequency oscillations in phase and amplitude distribution of the gratings, which makes the designed LPGs rarely to be realized in practice. Hereafter, we will propose and demonstrate an analysis method for design of the LPG-based edge filter. Without loss of the generalities, the grating is assumed to be weak one (i.e., all the coupling coefficients $\kappa(z)$ are assumed to be small magnitudes), in the first order Born approximation, the cross-transmission coefficient $c(\delta)$ has the Fourier transform relationship with the complex coupling coefficient $\kappa(z)$ and can be expressed by

$$c(\delta) = i \int_{-\infty}^{\infty} \kappa^*(z) \exp(-i2\delta z)dz, \tag{6}$$

where κ and δ have the same meaning as those in (2). The complex coupling coefficient $\kappa(z)$ can be further divided into the amplitude and the phase parts and written by

$$\kappa(z) = |\kappa(z)| \exp(i\varphi(z)), \tag{7}$$

where $\varphi(z)$ represents the grating phase. Substituting (7) into (6), then the cross-transmission function can be approximately expressed as

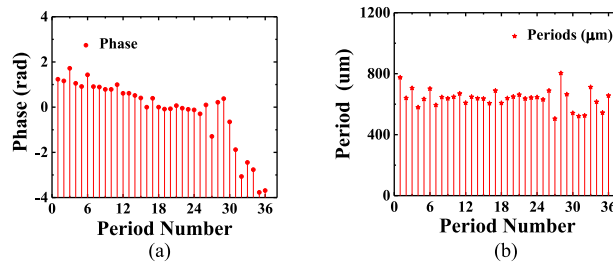$$c(\delta) \propto c_A(\delta) \otimes c_P(\delta), \tag{8}$$

Fig. 1. Optimal results for the phases and periods of the required edge filter. (a) The optimal phases, and (b) the corresponding periods of the LPG.

and

$$c_A(\delta) = i \int_{-\infty}^{\infty} |\kappa(z)| \exp(-i2\delta z) dz, \tag{9}$$

$$c_P(\delta) = i \int_{-\infty}^{\infty} \exp(-i\varphi(z)) \exp(-i2\delta z) dz, \tag{10}$$

where $\otimes$ represents the convolution operation. From the (8)–(10), it is seen that for any given target of the cross-transmission spectrum $c(\delta)$, it can be regarded as a convolution of two independent parts: $c_A(\delta)$ and $c_p(\delta)$. The former one is the Fourier transform of the grating's amplitude, and the latter one is the Fourier transform of the grating's phase. For most of the previous designs [23]–[25], only the amplitude part of the coupling coefficient is considered and optimized. If phase part of the coupling coefficient could also be optimized, which may help us to find a better design enabling to avoid the above fabrication problems. For example, one can purposely set the amplitude of the coupling coefficient in (9) as a constant (the grating becomes the so-called uniformly apodized LPG), $c_A(\delta)$ is then a Delta function, and then the target spectrum $c(\delta)$ can be approximately regarded as the spectrum $c_P(\delta)$, which is only dependent on the grating's phase. In concrete, the phase distribution $\varphi(z)$ can be easily reconstructed from the (10) by doing the inverse Fourier transform. Here we call this kind of gratings the phase-only modulated ones, which may considerably decrease the fabrication difficulties of the gratings, especially for LPG-based edge filter in which a triangular-type spectrum is particularly demanded. Idea of which was previously proposed in [26] and [27] for the design of the FBG-based multiple-channel filter and the pulse shaping devices. In the following, we will employ this method for the design of LPG-based edge filters.

2.3 Spectrum Objective and Merit Function of the Edge Filter

In the following simulation, the central period and total length of the LPG-based edge filter are particularly chosen as 0.648 mm and 23.328 mm (i.e., 36 periods), respectively. Parameters of the utilized fiber such as the diameters of the core a_1 and cladding a_2, the refractive indices of the core n_1 and cladding n_2, and the surrounding material n_3, are particularly chosen as: $a_1 = 8.2\,\mu m$, $a_2 = 125\,\mu m$, $n_1 = 1.4580$, $n_2 = 1.4536$, and $n_3 = 1.0$. As discussed in most of the previous papers [10]–[21], only the amplitude spectrum is considered in edge-filter interrogation scheme. Moreover, the objective function for the transmission spectrum of the edge filter is given as:

$$O(\lambda) = \begin{cases} T_B + \frac{T_B - T_E}{\lambda_B - \lambda_E}(\lambda - \lambda_B), & \lambda_B \le \lambda \le \lambda_E \\ 1, & \text{others} \end{cases}, \tag{11}$$

where the maximum and minimum transmission T_B and T_E are chosen as 1 and 0.15, respectively, and the corresponding wavelength are chosen as $\lambda_B = 1540$ nm, $\lambda_E = 1590$ nm, respectively. The objective spectrum above will be plotted as "OF" in Fig. 2 for comparing with the designed edge filter. Unlike the edge filter's designs reported in [19]–[21] where an objective function including two declined edges is generally adopted, here without losing any functionalities of the edge filter for
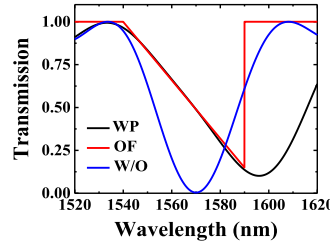
Fig. 2. Simulation results for the transmission spectra of the LPGs, where the curves OF, WP, and W/O represent the target, the calculated spectra with and without phase inserted, respectively.

the intensity-interrogation scheme [12], [14], [17], only one-side edge filter is considered and used as the objective function. We have found that this selection provides more flexibilities and would considerably facilitate to obtain better design results. Moreover, it must be noted that for the design of FBG, since the period is pretty small ($\sim$0.5 μm), the number of the period is so large ($>10^5$) that it is hard or even impossible to optimize phases of the coupling coefficients in all periods. However, for LPG design, since the period ($\sim$0.6 mm) is much larger than that of FBG, number of the period is very limited and thus one can directly optimize the phase of coupling coefficient in each period. In this design, the target LPG is assumed to have 36 periods, which indicates that the number of the phases required to optimize is just 36 for the phase-only modulated LPG, and their complex coupling coefficients can be simply expressed by:

$$\kappa_j = |\kappa| \exp(j\varphi_j), \qquad 1 \leq j \leq M = 36 \qquad (12)$$

where φ_j represents phase of the coupling coefficient at jth period, $|\kappa|$ is amplitude of the coupling coefficient, which is assumed to be a constant in this study. Once if all the phase terms φ_j are determined, then by using the (2)–(5), transmission spectrum of the designed LPG can be calculated.

To well evaluate the linearity of the designed edge filter, we make use of the normalized root-mean-square error (NRMSE) as the merit function, which is defined by:

$$\text{NRMSE}_O = \sqrt{\sum_{i=1}^{N} |S(\lambda_i) - O(\lambda_i)|^2} / \sqrt{\sum_{i=1}^{N} |O(\lambda_i)|^2}, \qquad (13)$$

where $N = (\lambda_E - \lambda_B)/d_\lambda + 1$, indicates number of the samples and d_λ is the spectral resolution. $O(\lambda_i)$ is the discrete target spectrum given by (11). $S(\lambda_i)$ is the calculated spectrum. Moreover $\lambda_1 = \lambda_B$ and $\lambda_N = \lambda_E$ are assumed here. For calculation, the wavelength range and the spectral resolution were chosen as the ones ranging from 1540 nm to 1590 nm and 0.05 nm, respectively. In order to find the optimal phase terms φ_j with which the NRMSE$_o$ (defined by (13)) becomes the minimum, one can make use of the multiple-objective-optimization (MOO) algorithms, such as the genetic algorithm (GA) [24], the simulated annealing algorithm [25], [26], or the other nonlinear optimization methods. In this study, we have adopted the genetic algorithm to find the best solutions for (13). However, the detailed explanations about this algorithm are neglected here, which in fact can be found elsewhere in [24].

3. Simulation Results and Discussions

While the genetic algorithm is utilized, too large or too small population size (number of the phase in our case) cannot achieve good optimization results [30]. Here 36 periods (i.e., 36 phases) of the LPG is particularly selected in this study, and optimization for the 36 phases have been performed. The results are shown in Fig. 1(a). In addition, the obtained phase function φ shown in Fig. 1(a) can be equivalently turned into the local pitches of the LPG by

$$\Lambda_j = \Lambda_0 \left(1 + \Delta\varphi_j/2\pi\right), \qquad 1 \leq j \leq M = 36, \qquad (14)$$

TABLE 1

Properties of the Edge Filters Obtained by Using Different Methods

Methods	Dynamic range (Wavelength)	Dynamic range (Loss)
Phase-only modulated LPG	50 nm	~85%
Multimode fiber (MMF) [10]	~2 nm	~25%
Erbium-doped fiber (EDF) [11]	10 nm	~90%
Uniform LPG [12]	7.5 nm	~80%
1550/1570 WDM [13]	1 nm	~90%
Ultra-long-period fiber grating [14]	10nm	~90%
FBG with cladding mode coupling [16]	10 nm	~75%
Uniform helical LPG [17]	10 nm	~75%
Apodized linearly chirped FBG [18]	10 nm	60%
FBG synthesized by the genetic algorithm (GA) [19]	5 nm	~80%
FBG using covariance matrix adapted evolution algorithm [20]	1.8 nm	~90%
FBG using DLP algorithm [21]	~0.1 nm	~90%

where Λ_0 ($= 648 \ \mu$m in our case) is the nominal pitch of the grating without any phase modulation. $\Delta\varphi_j = \varphi_j - \Delta\varphi_{j-1}$ is the phase change and the initial phase change is assumed to be φ_1 ($\Delta\varphi_1 = \varphi_1$). The corresponding pitches required for all the 36 periods are shown in Fig. 1(b). From this figure, it can be seen that due to the introduction of the phase-only modulation, the grating pitches are no longer constant, which become variable at different local positions.

Then the corresponding spectra are calculated, which is shown in Fig. 2 and labeled by "WP". For comparison purpose, the objective function for the transmission spectrum $O(\lambda)$ (11) and transmission spectrum for the conventional LPG (i.e., all the φ_j are assumed to be zeroes) are also depicted in Fig. 2, which are labeled by "OF" and "W/O", respectively. From Fig. 2, it is seen that the spectrum of the designed filter agrees well with the objective one (11) at wavelengths ranging from 1540 to 1590 nm, and the linear transmission-loss region obtained is about ~85%, which indicates that the designed edge filter completely meets the target that we set in advance.

To further evaluate the designed edge-filter that we have obtained, especially for the performances such as the linear wavelength range and the linear transmission-loss range, most of the edge filters previously obtained with different methods had been investigated. The comparison results are summarized in Table 1. From this table, it can be seen that the edge filter obtained in this study has a dynamic wavelength range of ~50 nm, which is the at least 5 times larger than best of the other results. Meanwhile the dynamic range in transmission loss obtained in this study is about 85%, which is even better than the previous ones reported to date.

4. Tolerance Analyses for the Designed Edge Filter

4.1 Effect of the Coupling-Coefficients Amplitude on the LPG's Spectrum

The optimal design shown in Fig. 2 are obtained under the conditions that both the grating length and the amplitude of the coupling coefficients are kept constants. In the real fabrication processes,
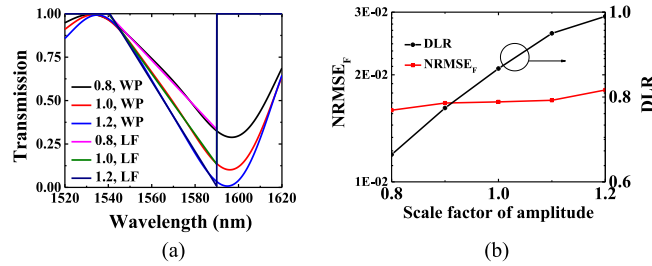
Fig. 3. Simulation results for effects of the grating's strength on the resulted spectrum. (a) Transmission spectra, and (b) the corresponding NRMSE$_F$ and DLR results.

in general the strength (amplitude of the coupling coefficients) of the resulted LPGs cannot be guaranteed to have the same value as what we pre-assumed in design, which inevitably would result in some changes in the loss-depth of the resulted filter. Therefore, it is reasonable to expect that when the amplitude of the coupling coefficients changes, the slope of the obtained edge filter will change accordingly. Meanwhile the obtained linear-region will also be changed. To evaluate the linear performance of the newly resulted spectrum, the new merit function (NRMSE) is utilized, which can be expressed as:

$$\text{NRMSE}_F = \sqrt{\sum_{i=1}^{N} |S(\lambda_i) - F(\lambda_i)|^2} / \sqrt{\sum_{i=1}^{N} |F(\lambda_i)|^2}, \tag{15}$$

where unlike the $O(\lambda_i)$ in (13) which is the target spectrum, $F(\lambda_i)$ is a new function which is directly obtained by linearly fitting the curve $S(\lambda_i)$ at wavelengths ranging from λ_B to λ_E. Therefore, NRMSE$_F$ actually represents the ripple quantity, which enables to evaluate the linearity of the resulted spectrum $S(\lambda_i)$. Fig. 3(a) shows the calculated results for transmission spectra of three different edge filters which have the same phases but different amplitudes of the coupling coefficients. For comparisons, their linear fitting curve are also shown in Fig. 3(a), where the labels of "0.8","1.0", and "1.2" represent the gratings while their strength are 80%, 100%, and 120% percent of the designed one. "WP" and "LF" represent the spectra of the designed filter and its linear fitting curve, respectively.

From Fig. 3(a), it is seen that with increment in the grating strength, the slope of designed edge filter increases and wider dynamic transmission-loss range can be obtained. Meanwhile the linearity of the three edge filters change a little. To further make sure that the above results, the values of NRMSE$_F$ (i.e., (15)) and the corresponding dynamic transmission-loss range (DLR) in terms of the different grating strengths have also been investigated, results of which are shown in Fig. 3(b). From this Figure, it can be seen that when the grating strength increases, the DLRs will accordingly increase but meanwhile linearity of the designed edge filter (i.e., NRMSE$_F$) will inevitably become worse. So we need to make a trade-off for the requirement of both a broader dynamic range and a smaller NRMSE$_F$. The above results in return mean that if the grating strength can be controlled with $\pm20\%$ of its preset one, the deviation effects on the spectrum of the edge filter could be neglected.

4.2 Effects of the Coupling Coefficient Deviations on the LPG's Spectrum

During the practical fabrication process of a LPG, it is difficult to avoid the deviation of the amplitude in grating's coupling coefficient. Effects of the amplitude deviation on the spectrum of the designed filter have been investigated numerically. The results are shown in Fig. 4(a), where the curve labeled by "WP" represents the original designed spectra obtained without any deviations. The curves labeled "10%" and "20%" represent the spectra where there exist $\pm10\%$ and $\pm20\%$ random amplitude deviations (uniform distribution) in each period of the grating. "LF" represents the fitting curve of "WP". Moreover, the corresponding NRMSE$_F$s have been calculated, which are shown in Fig. 4(b). Noted that for random amplitude deviation, it will result in random changes in spectrum, so here we apply Monte Carlo statistical method to obtain the statistical spectrum and the corresponding NRMSE$_F$ as shown in Fig. 4(b), which are obtained by averaging the 1000 different ones.
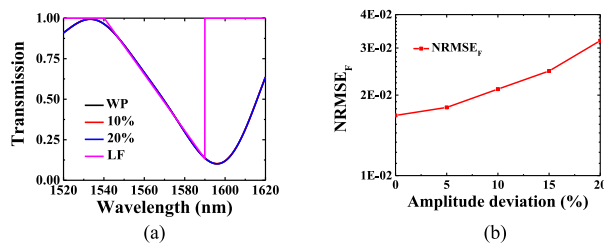
Fig. 4. Simulation results for effects of the amplitude deviations on the resulted spectra. (a) Transmission spectra, and (b) the corresponding NRMSE$_F$ results.
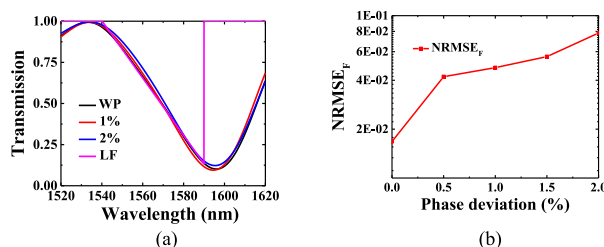

Fig. 5. Simulation results for effects of the phase deviations on the resulted spectra. (a) Transmission spectra, and (b) the corresponding NRMSE$_F$ results.

From Fig. 4, it can be seen that the spectrum and the corresponding NRMSE$_F$ of the resulted edge filter changes a little even if the amplitude-deviation is larger than $\pm 20\%$, which in return indicates that the designed edge filter is very robust to the fluctuations resulted in the grating's amplitude during the fabrication process.

The spectral effects of the imperfection phases in the coupling coefficients have also been investigated, the results are shown in Fig. 5(a), where the curve labeled by "WP" represents the original designed spectra obtained without any deviations. The curves labeled by "1%" and "2%" represent the spectra where there exist $\pm 1\%$ and $\pm 2\%$ random phase deviation in each period. "LF" represents the fitting curve of "WP", which is as same as that fitting curve in Fig. 4. For same reason, we also apply the Monte Carlo statistical method to obtain the statistical data of the NRMSE$_F$ as shown in Fig. 5(b), which are obtained by averaging the 1000 different ones.

From Fig. 5(a), it can be seen that the phase imperfection even with $\pm 1\%$ deviation to the designed magnitude will strongly affect the resulted spectrum. Moreover, comparing Fig. 5(b) with Fig. 4(b), the NRMSE$_F$ caused by phase deviation is about ten times larger than that caused by the amplitude deviation, which in return means that in order to well fabricate the phase-only modulated LPG, one should precisely control the phases with a deviation tolerance of less than $\pm 1\%$ to their nominal magnitudes. Fortunately, periods of the LPGs considered in this study are among the several hundred micrometers (see the data in Fig. 1(b)), $\pm 1\%$ phase deviation just corresponds to a deviation of ± 6 μm in grating period, which is acceptable and realizable by using the current LPG's fabrication platform in [28] and [29], because the commercial translation stage nowadays can easily have a position accuracy up to 0.25 μm, which completely meet the fabrication tolerance demanded for our designs.

5. Conclusion

We have proposed and demonstrated an efficient method for designing an edge filter with ultra-wide dynamic range, which is realized based on a phase-only modulated long-period fiber grating (LPG). The designed edge filter has wavelength and transmission-loss dynamic ranges of about 50 nm and 85%, respectively, which are the best results reported to date according to the best knowledge of the authors. The simulation results also show that the phase deviation will strongly affect the

linearity of the obtained filter. However, if the phase deviations can be controlled within $\pm1\%$ of the nominal magnitudes, the distortion effect can nearly be neglected. For LPG's fabrication, $\pm1\%$ deviation in phase is equivalent to a deviation of $\pm6~\mu\mathrm{m}$ in grating period for our design, which is however realizable according to the current LPG's fabrication platform.

References

[1] V. Bhatia and A. Vengsarkar, "Optical fiber long-period grating sensors," *Opt. Lett.*, vol. 21, no. 9, pp. 692–694, 1996.

[2] H. Patrick, A. Kersey, and F. Bucholtz, "Analysis of the response of long period fiber gratings to external index of refraction," *J. Lightw. Technol.*, vol. 16, no. 9, pp. 1606–1612, Sep. 1998.

[3] V. Bhatia, "Applications of long-period gratings to single and multi-parameter sensing," *Opt. Exp.*, vol. 4, no. 11, pp. 457–466, 1999.

[4] L. Zhang, Y. Liu, L. Everall, J. Williams, and I. Bennion, "Design and realization of long-period grating devices in conventional and high birefringence fibers and their novel applications as fiber-optic load sensors," *IEEE J. Sel. Top. Quantum Electron.*, vol. 5, no. 5, pp. 1373–1378, Sep./Oct. 1999.

[5] S. James and R. Tatam, "Optical fibre long-period grating sensors: characteristics and application," *Meas. Sci. Technol.*, vol. 14, no. 5, pp. R49–R61, 2003.

[6] I. Villar, F. Arregui, I. Matias, A. Cusano, D. Paladino, and A. Cutolo, "Fringe generation with non-uniformly coated long-period fiber gratings," *Opt. Exp.*, vol. 15, no. 15, pp. 9326–9340, 2007.

[7] X. Chen, K. Zhou, L. Zhang, and I. Bennion, "Optical chemistry sensors utilizing long-period fiber gratings UV-inscribed in D-fiber with enhanced sensitivity through cladding etching," *IEEE Photon. Technol. Lett.*, vol. 16, no. 5, pp. 1352–1354, May 2004.

[8] R. Murphy, S. James, and R. Tatam, "Multiplexing of fiber-optic long-period grating-based interferometric sensors," *J. Lightw. Technol.*, vol. 25, no. 3, pp. 825–829, Mar. 2007.

[9] Y. Wang, L. Xiao, D. Wang, and W. Jin, "Highly sensitive long-period fiber-grating strain sensor with low temperature sensitivity," *Opt. Lett.*, vol. 31, no. 23, pp. 3414–3416, 2006.

[10] L. Wei, A. Khattak, C. Martz, and D. P. Zhou, "Tunable multimode fiber based filter and its application in cost-effective interrogation of fiber-optic temperature sensors," *IEEE Photon. J.*, vol. 9, no. 2, Apr. 2017, Art. no. 7101808.

[11] U. Tiwari, K. Thyagarajan, M. Shenoy, and S. Jain, "EDF-based edge-filter interrogation scheme for FBG sensors," *IEEE Sensors J.*, vol. 13, no. 4, pp. 1315–1319, Apr. 2013.

[12] V. Mamidi *et al.*, "Fiber Bragg grating-based high temperature sensor and its low-cost interrogation system with enhanced resolution," *Opt. Appl.*, vol. 44, no. 2, pp. 299–308, 2014.

[13] P. Wei, C. Cheng, L. Deng, and T. Liu, "An economical fiber Bragg grating interrogator for medium-scale sensing application," *IEEE Photon. Technol. Lett.*, vol. 28, no. 12, pp. 1306–1308, Jun. 2016.

[14] Y. Rao, T. Zhu, and Q. Mo, "Highly sensitive fiber-optic torsion sensor based on an ultra-long-period fiber grating," *Opt. Commun.*, vol. 266, no. 1, pp. 187–190, 2006.

[15] V. Dangui, M. Digonnet, and G. Kino, "Ultrabroadband single-mode long-period fiber gratings using high-order cladding modes," *J. Appl. Phys.*, vol. 96, no. 11, pp. 5987–5991, Dec. 2004.

[16] L. Xian, P. Wang, K. Ogusu, and H. Li, "Cladding mode coupling in a wide-band fiber Bragg grating and its application to a power-interrogated temperature sensor," *IEEE Photon. Technol. Lett.*, vol. 25, no. 3, pp. 231–233, Feb. 2013.

[17] L. Xian, P. Wang, and H. Li, "Power-interrogated and simultaneous measurement of temperature and torsion using paired helical long-period fiber gratings with opposite helicities," *Opt. Exp.*, vol. 22, no. 17, pp. 20260–20267, 2014.

[18] S. Bandyopadhyay, P. Biswas, A. Pal, S. K. Bhadra, and K. Dasgupta, "Empirical relations for design of linear edge filters using apodized linearly chirped fiber Bragg grating," *J. Lightw. Technol.*, vol. 26, no. 24, pp. 3853–3859, Dec. 2008.

[19] R. Huang, Y. Zhou, H. Cai, R. Qu, and Z. Fang, "A fiber Bragg grating with triangular spectrum as wavelength readout in sensor systems," *Opt. Commun.*, vol. 229, pp. 197–201, 2004.

[20] S. Baskar, P. N. Suganthan, N. Ngo, A. Alphones, and R. Zheng, "Design of triangular FBG filter for sensor applications using covariance matrix adapted evolution algorithm," *Opt. Commun.*, vol. 260, pp. 716–722, 2006.

[21] M. Li, J. Hayashi, and H. Li, "Advanced design of a complex fiber Bragg grating for a multichannel asymmetrical triangular filter," *J. Opt. Soc. Amer. B*, vol. 26, no. 2, pp. 228–234, 2009.

[22] T. Erdogen, "Fiber grating spectra," *J. Lightw. Technol.*, vol. 15, no. 8, pp. 1277–1294, Aug. 1997.

[23] J. K. Brenne and J. Skaar, "Design of grating-assisted codirectional couplers with discrete inverse-scattering algorithms," *J. Lightw. Technol.*, vol. 21, no. 1, pp. 254–263, Jan. 2003.

[24] R. Kritzinger and J. Meyer, "Design and fabrication of novel broadband using synthesis techniques," *J. Lightw. Technol.*, vol. 29, no. 8, pp. 1077–1084, Apr. 2011.

[25] H. Li and Y. Sheng, "Direct design of multichannel fiber Bragg grating with discrete layer-peeling algorithm," *IEEE Photon. Technol. Lett.*, vol. 15, no. 9, pp. 1252–1254, Sep. 2003.

[26] H. Li, M. Li, and J. Hayashi, "Ultrahigh-channel-count phase-only sampled fiber Bragg grating covering the S, C, and L bands," *Opt. Lett.*, vol. 34, no. 7, pp. 938–940, 2009.

[27] M. Preciado, X. Shu, and K. Sugden, "Proposal and design of phase-modulated fiber gratings in transmission for pulse shaping," *Opt. Lett.*, vol. 38, no. 1, pp. 70–72, 2013.

[28] P. Wang, L. Xian, and H. Li, "Fabrication of phase-shifted long-period fiber grating and its application to strain measurement," *IEEE Photon. Technol. Lett.*, vol. 27, no. 5, pp. 557–560, Mar. 2015.

[29] M. Partridge, S. James, J. H. Barrington, and R. Tatam, "Overwrite fabrication and tuning of long period gratings," *Opt. Exp.*, vol. 24, no. 20, pp. 22345–22356, 2016.

[30] J. Grefenstette, "Optimization of control parameters for genetic algorithm," *IEEE Trans. Syst. Man. Cybern.*, vol. SMC-16, no. 1, pp. 122–128, Jan. 1986.